

Propagation of Uncertainties Modelled by Parametric P-boxes Using Sparse Polynomial Chaos Expansions

Roland Schöbi

Ph.D. student, Chair of Risk, Safety and Uncertainty Quantification, ETH Zurich, Zurich, Switzerland

Bruno Sudret

Professor, Chair of Risk, Safety and Uncertainty Quantification, ETH Zurich, Zurich, Switzerland

ABSTRACT: Advanced simulations, such as finite element methods, are routinely used to model the behaviour of physical systems and processes. At the same time, awareness is growing on concepts of structural reliability and robust design. This makes efficient quantification and propagation of uncertainties in computation models a key challenge. For this purpose, surrogate models, and especially Polynomial Chaos Expansions (PCE), have been used intensively in the last decade. In this paper we combine PCE and probability-boxes (p-boxes), which describe a mix of aleatory and epistemic uncertainty. In particular, parametric p-boxes allow for separation of the latter uncertainties in the input space. The introduction of an augmented input space in PCE leads to a new uncertainty propagation algorithm for p-boxes. The proposed algorithm is illustrated with two applications: a benchmark analytical function and a realistic truss structure. The results show that the proposed algorithm is capable of predicting the p-box of the response quantity extremely efficiently compared to double-loop Monte Carlo simulation.

1. INTRODUCTION

In modern engineering sciences, computational simulations, such as finite element modelling, have become wide spread. The goal is to predict the response of a system with respect to a set of parameters, *e.g.* the deflection of a beam under variable loads. The parameters (*e.g.* geometries, mechanical properties, loads) are mapped to the quantity of interest through a computational model, *e.g.* through the governing equations of the process.

It is only in recent times that the traditionally deterministic model parameters have been gradually substituted with probability distributions that account for their uncertainty. In practice though, data available for calibrating such distributions are often too sparse, thus resulting in an extra layer of uncertainty in their parameters. Different frameworks have been proposed to quantify the latter lack of knowledge (epistemic uncertainty) as well as the natural variability of the process (aleatory

uncertainty), including probability-boxes (Ferson and Ginzburg, 1996), Bayesian hierarchical models (Gelman, 2006) and Dempster-Shafer's evidence theory (Dempster, 1967; Shafer, 1976). These frameworks are generally referred to as *imprecise probabilities*.

After the input uncertainty is characterized, it must be propagated through a computational model. The latter, however, is often an expensive-to-evaluate function, which can be replaced by an approximate model, *i.e.* a meta-model, to reduce the computational effort needed. Well-known meta-modelling techniques include Polynomial Chaos Expansions (Ghanem and Spanos, 2003), Gaussian process modelling (a.k.a. Kriging) (Santner et al., 2003) and support vector machines (Gunn, 1998).

This paper describes one formulation of imprecise probabilities in Section 2 followed by an introduction to Polynomial Chaos expansions in Section 3. Finally these two ingredients are combined

in Section 4 and two applications are discussed in Section 5.

2. INPUT UNCERTAINTY

2.1. Probability theory

Traditionally, uncertainty in engineering has been treated with probability theory.

Consider a probability space $(\Omega, \mathcal{F}, \mathbb{P})$, where Ω denotes the event space equipped with σ -algebra \mathcal{F} and probability measure \mathbb{P} . Random variables are denoted by capital letters $X(\omega) : \Omega \rightarrow \mathcal{D}_X \subset \mathbb{R}$ where $\omega \in \Omega$. A realization of variable X is denoted by the corresponding lower case letters, e.g. x . Several random variables compose a random vector $\mathbf{X} = [X_1, \dots, X_M]^T$ and the corresponding realizations $\mathbf{x} = [x_1, \dots, x_M]^T$.

In this context a random variable X is described by its *cumulative distribution function* (CDF) F_X which expresses the probability that $X < x$, i.e. $F_X(x) = \mathbb{P}(X < x)$. The CDF has the properties that it is monotone non-decreasing, that it tends to zero for low values of x ($F_X(x \rightarrow -\infty) = 0$) and that it tends to one for high values of x ($F_X(x \rightarrow \infty) = 1$). Note that such properties are valid for continuous as well as discrete random variables.

For continuous random variables, the derivative of a CDF is the *probability density function* $f_X(x) = dF_X(x)/dx$. The PDF describes the likelihood that X is in the neighbourhood of x . Due to the fact that the CDF is non-decreasing, the PDF has non-negative values for all $x \in X$.

As seen in the definitions above, probability theory offers a single measure (i.e. the probability measure) to describe variability in variable X . In other words, we assume that the variability in X is known and quantifiable by the CDF F_X and the corresponding PDF f_X . This describes the case where variability is treated as the only source of uncertainty.

2.2. Probability-box

A more general formulation is given by the framework of *probability-boxes* (p-boxes) which defines the CDF of a variable X by its lower and upper bound distributions (Ferson and Ginzburg, 1996; Ferson and Hajagos, 2004). The idea is that due a lack of knowledge (epistemic uncertainty), the CDF

cannot be given a precise formulation. Thus the probability-box framework accounts for aleatory as well as for epistemic uncertainty in the description of a variable X .

The lower and upper boundaries of the CDF are denoted by $[F_X, \bar{F}_X]$. The true, but unknown, CDF of X lies within the boundaries for any value of $x \in X$, i.e. $F_X(x) \leq F_X(x) \leq \bar{F}_X(x)$, $\forall x \in X$. The boundaries $[F_X, \bar{F}_X]$ mark the extreme cases of F_X and are thus also CDFs by definition.

The two boundaries form an intermediate space in the variable-CDF-graph which resembles a box (see Figure 1), hence the name probability-box.

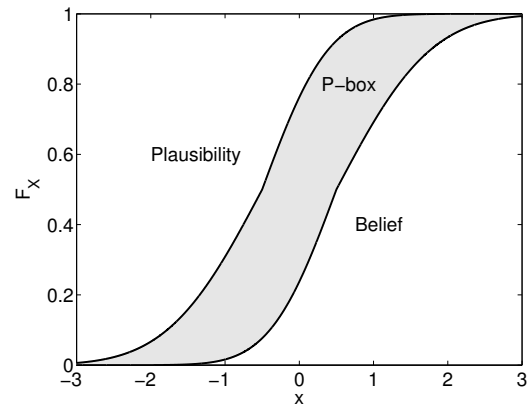


Figure 1: P-box – CDF of a Gaussian variable with interval-valued μ_X and σ_X

The p-box can be interpreted in the framework of *Dempster-Shafer's evidence theory* (Dempster, 1967; Shafer, 1976). The lower boundary F_X describes the minimum amount of probability that *must* be assigned to $F_X(x)$, which corresponds to the *belief* function $\text{Bel}(F_X(x))$ in the vocabulary of evidence theory. Analogously, the upper boundary of the p-box is associated with the maximum amount of probability that *might* be assigned to $F_X(x)$, or the *plausibility* function $\text{Pl}(F_X(x))$.

Note that if $F_X(x) = F_X(x) = \bar{F}_X(x)$, $\forall x \in X$, then the p-box is called *thin* and conventional probability theory can be applied.

2.3. Parametric p-boxes

In the literature two types of p-boxes are identified, namely the *free p-box* and the *parametric p-box*. In this paper, we focus on parametric p-boxes (also called *distributional p-boxes*).

A *parametric p-box* requires knowledge about the shape of the true CDF but allows for uncertainty in its parameters. The p-box is represented by a family of distribution functions whose parameters θ lie within an interval. For a single variable X :

$$F_X(x) = F_X(x, \theta), \quad (1)$$

where $\theta_i \in [\underline{\theta}_i, \bar{\theta}_i]$, $i = 1, \dots, n_\theta$. This construction resembles a Bayesian hierarchical model (Gelman, 2006) in which the distribution of the parameters θ is replaced by an interval. This framework allows for a clear separation of aleatory and epistemic uncertainty: aleatory uncertainty is represented by the distribution function family and epistemic uncertainty is represented by the interval on parameters θ .

Figure 2 illustrates a parametric p-box generated by a Gaussian random variable with mean value and standard deviation varying within the intervals $\mu_X = [-0.5, 0.5]$ and $\sigma_X = [0.7, 1.0]$. Several realizations of the CDF are shown. Note that in the case of parametric p-boxes in general, lower/upper boundaries of the p-box are composed of several realizations of the p-box.

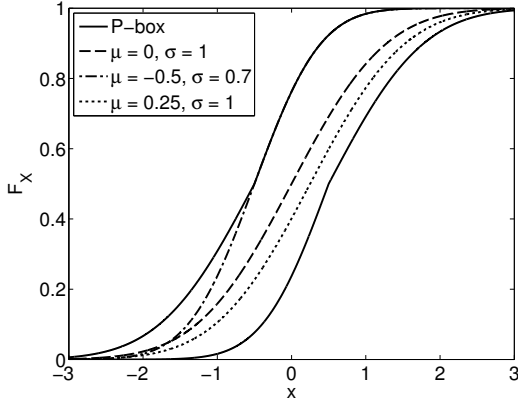


Figure 2: Boundaries of a parametric p-box and some realizations for specific parameter values θ^*

3. META-MODELLING

3.1. Computational model

A computational model \mathcal{M} is defined as a mapping of the M -dimensional input vector \mathbf{x} to the output scalar y , i.e. $\mathcal{M} : \mathbf{x} \in \mathcal{D}_X \subset \mathbb{R}^M \rightarrow y \in \mathbb{R}$. Due to uncertainties in the input vector, the latter is represented by the random vector \mathbf{X} with joint CDF F_X .

The components of $\mathbf{X} = [X_1, \dots, X_M]^T$ are assumed independent for the sake of simplicity throughout this paper. The model response is a random variable Y obtained by propagating the input random vector \mathbf{X} through the computational model \mathcal{M} .

Several techniques are available for surrogating the expensive-to-evaluate computational model \mathcal{M} . In the following section, Polynomial Chaos Expansions (Ghanem and Spanos, 2003; Sudret, 2007) will be briefly introduced.

3.2. Polynomial Chaos Expansion

A well-known non-intrusive meta-modelling method is *Polynomial Chaos Expansion* (PCE) which approximates the computational model \mathcal{M} with a finite series of polynomials orthogonal with respect to the distribution of the input variables:

$$Y \approx \mathcal{M}^{(PCE)}(\mathbf{X}) = \sum_{\alpha \in \mathcal{A}^{M,p}} a_\alpha \psi_\alpha(\mathbf{X}), \quad (2)$$

where $\{a_\alpha \in \mathbb{R}\}$ are the polynomial coefficients for the multi-indices $\alpha = [\alpha_1, \dots, \alpha_M]$ in the truncation set $\mathcal{A}^{M,p}$, M is input dimension, p is the maximum polynomial degree and $\psi_\alpha(\mathbf{X})$ are multivariate orthonormal polynomials. Since the components of \mathbf{X} are assumed independent, the joint PDF is the product of the marginals. For each marginal distribution f_{X_i} a functional inner product is defined:

$$\langle \phi_1, \phi_2 \rangle_i = \int_{\mathcal{D}_i} \phi_1(x) \phi_2(x) f_{X_i}(x) dx. \quad (3)$$

For each input variable $i = 1, \dots, M$ a family of orthonormal polynomials can be built that satisfies:

$$\langle \psi_j^{(i)}, \psi_k^{(i)} \rangle = \int_{\mathcal{D}_i} \psi_j^{(i)}(x) \psi_k^{(i)}(x) f_{X_i}(x) dx = \delta_{jk}, \quad (4)$$

where δ_{jk} is the Kronecker symbol which is $\delta_{jk} = 1$ for $j = k$ and $\delta_{jk} = 0$ otherwise. A compilation of common orthonormal univariate polynomials can be found e.g. in Sudret (2014).

3.3. Sparse PCE

One strategy to compute efficiently the coefficients a_α in Eq. (2) is linear regression, as introduced by Berveiller et al. (2006). Consider a set of N samples of the input vector $\mathcal{X} = \{\chi^{(1)}, \dots, \chi^{(N)}\}$, known

as the *experimental design*, and the corresponding responses of the exact computational model $\mathcal{Y} = \left\{ \mathcal{Y}^{(1)} = \mathcal{M}(\boldsymbol{\chi}^{(1)}), \dots, \mathcal{Y}^{(N)} = \mathcal{M}(\boldsymbol{\chi}^{(N)}) \right\}$. The set of coefficients $a_{\boldsymbol{\alpha}}$ can be computed through the solution of the least squares problem:

$$\hat{\mathbf{a}} = \arg \min_{\mathbf{a} \in \mathbb{R}^{|\mathcal{A}|}} \frac{1}{N} \sum_{i=1}^N \left(\mathcal{Y}^{(i)} - \sum_{\boldsymbol{\alpha} \in \mathcal{A}^{M,p}} a_{\boldsymbol{\alpha}} \psi_{\boldsymbol{\alpha}}(\boldsymbol{\chi}^{(i)}) \right)^2. \quad (5)$$

The efficiency of meta-modelling algorithms depends greatly on the choice of the set of polynomials $\mathcal{A}^{M,p}$ (see Eq. (5)). Different strategies for limiting the number of polynomials have been proposed including hyperbolic index sets (Blatman and Sudret, 2011) which limit the total degree of polynomials and interactions. In case of high dimensionality ($M \uparrow$) this truncation scheme is not efficient enough to accurately estimate the model response Y and at the same time have a small number of elements in $\mathcal{A}^{M,p}$.

For this reason, algorithms have been developed to select out of a candidate set the polynomials that are most influential to the system response Y . Following Efron et al. (2004), Blatman and Sudret (2010) introduced the *least angle regression selection* (LARS) algorithm for this purpose. LARS determines the sparse set of polynomials (out of a candidate set) that best describes the behaviour of the exact computational model based on the experimental design.

4. UNCERTAINTY PROPAGATION OF P-BOXES

4.1. Monte-Carlo-based propagation

The distinction of aleatory and epistemic uncertainty in the formulation of the parametric p-box allows one to propagate them separately. A straightforward algorithm is the *nested Monte Carlo algorithm* (Eldred and Swiler, 2009; Chowdhary and Dupuis, 2013) shown in Figure 3. In the outer loop, parameters of the CDF are sampled, *i.e.* $\boldsymbol{\theta}^{(i)} \in \Theta_{\mathbf{X}}$. In the inner loop, a Monte Carlo simulation is conducted for estimating the CDF of the response value Y for a given input distribution $F_{\mathbf{X}}(\mathbf{x}, \boldsymbol{\theta})$. The set of CDFs resulting from different values of $\boldsymbol{\theta}^{(i)}$ are finally combined into a p-box. The boundaries of the

p-box are obtained by:

$$\underline{F}_Y(y) = \min_i \left(F_Y(y, \boldsymbol{\theta}^{(i)}) \right), \quad \forall y \in \mathcal{D}_Y \quad (6)$$

$$\overline{F}_Y(y) = \max_i \left(F_Y(y, \boldsymbol{\theta}^{(i)}) \right), \quad \forall y \in \mathcal{D}_Y. \quad (7)$$

The nested Monte Carlo approach requires a large number of model evaluations to accurately predict the p-box of the output variable Y . Thus the algorithm becomes inefficient when the cost for evaluating the computational model \mathcal{M} becomes large. Therefore we propose an algorithm to replace the computational model \mathcal{M} by its inexpensive-to-evaluate PCE surrogate.

4.2. PCE-based p-box propagation

4.2.1. Augmented input space

Consider the parametric p-box from Section 2.3, which separates aleatory and epistemic uncertainty. The response of the computational model Y can be interpreted as a function of the *augmented input vector* $\mathbf{Z} \stackrel{\text{def}}{=} [\mathbf{X}, \Theta_{\mathbf{X}}]^T$, where $\Theta_{\mathbf{X}}$ describes the space of all parameters of all marginal distributions, *e.g.* $\prod_{i=1}^M [\underline{\theta}_i, \overline{\theta}_i]$, if the p-box of each X_i depends on a single parameter θ_i . The augmented input space leads to a PCE of dimension $M_Z = M + |\Theta_{\mathbf{X}}|$ where $|\Theta_{\mathbf{X}}|$ is the number of parameters:

$$\mathfrak{Y} = \mathcal{M}^{(\text{aug})}(\mathbf{X}, \Theta_{\mathbf{X}}) = \mathcal{M}^{(\text{aug})}(\mathbf{Z}). \quad (8)$$

Note that the parameters $\{\theta_i, i = 1, \dots, n_{\theta}\}$ are given within interval boundaries $[\underline{\theta}_i, \overline{\theta}_i]$ and are treated in the PC expansion framework as a *uniformly distributed* random variable within these boundaries.

PCE is defined on independent random variables in the input space of the computational model, which is clearly not the case for parametric p-boxes because \mathbf{X} is depending on the parameters $\Theta_{\mathbf{X}}$. Thus an isoprobabilistic transform (*e.g.* *Nataf transform*) of the augmented input space is required before calibrating the meta-model (Blatman and Sudret, 2010).

For illustration purposes, the case of a Gaussian distribution is shown in this paper. Consider a parametric p-box of a Gaussian random variable X with unknown mean value μ_X and standard deviation

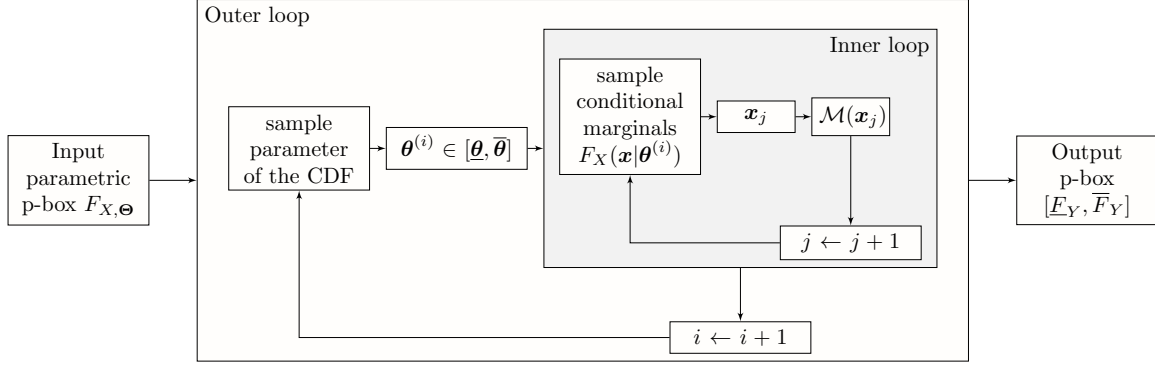


Figure 3: Nested Monte Carlo approach – Propagation of imprecise probabilities by sampling the parameters θ (outer loop) and the input vectors $\mathbf{x} \sim F_{\mathbf{X}}(\mathbf{x}, \theta)$ (inner loop)

σ_X , denoted by $X \sim \mathcal{N}([\underline{\mu}_X, \bar{\mu}_X], [\underline{\sigma}_X, \bar{\sigma}_X])$. The isoprobabilistic transform T reads:

$$X = \mu_X + \xi \cdot \sigma_X = U_1 + U_2 \cdot U_3, \quad (9)$$

where $U_1 = \mathcal{U}(\underline{\mu}_X, \bar{\mu}_X)$ and $U_2 = \mathcal{U}(\underline{\sigma}_X, \bar{\sigma}_X)$ denote uniform random variables between the two arguments and $\xi \stackrel{\text{def}}{=} U_3 = \mathcal{N}(0, 1)$ is a standard normal random variable.

The computational model can then be formulated as a function of three independent random variables:

$$Y = \mathcal{M}(X) = \mathcal{M}(T(U_1, U_2, U_3)), \quad (10)$$

where T is shown in Eq. (9).

Finally, the nested Monte Carlo algorithm described in Section 4.1 can be applied by substituting the full computational model $\mathcal{M}(\mathbf{X})$ with its surrogate in the augmented space $\mathcal{M}_{\text{PCE}}^{(\text{aug})}(\mathbf{Z})$.

4.2.2. Phantom points

Eq. (9) leads to an interesting feature of the experimental design in the augmented space. The computational model \mathcal{M} is a function of $|\mathbf{X}| = M$ variables whereas the augmented input space has $M_Z > M$ input variables. Hence, for a given $x \in \mathcal{D}_X$ there are several combinations of $\{u_1, u_2, u_3\}$ such that $u_1 + u_2 \cdot u_3 = x$. This feature can be exploited when generating the experimental design of PC expansion models in the augmented space.

Consider input variable X_j and the associated j -th component of the experimental design, i.e. $\mathcal{X}_j = \{\chi_j^{(1)}, \dots, \chi_j^{(N)}\}$. Each $\chi_j^{(k)} \in \mathcal{D}_{X_j}$ is a realization of the Normal distribution $\chi_j^{(k)} \sim \mathcal{N}(u_{1,j}^{(k)}, u_{2,j}^{(k)})$. It can then be described as a function of the variables in the augmented input space, i.e. $\chi_j^{(k)} = T(u_{1,j}^{(k)}, u_{2,j}^{(k)}, u_{3,j}^{(k)})$. Eq. (9) indicates that for Gaussian variables it holds:

$$u_{3,j}^{(k)} = \frac{\chi_j^{(k)} - u_{1,j}^{(k)}}{u_{2,j}^{(k)}}. \quad (11)$$

Thus for each sample $\chi_j^{(k)}, u_{3,j}^{(k)}$ can be computed as a function of $\{u_{1,j}^{(k)}, u_{2,j}^{(k)}\}$.

We define *phantom points* in the augmented input space as points which are obtained by sampling $\{u_{1,j}^{(k)}, u_{2,j}^{(k)}\}$ and computing $u_{3,j}^{(k)}$ by Eq. (11) resulting in the vector $\mathbf{u}_j^{(k)(i)} = \{u_{1,j}^{(k)(i)}, u_{2,j}^{(k)(i)}, u_{3,j}^{(k)(i)}\}$, where $i = 1, \dots, n_{ph}$. Combining the $j = 1, \dots, M$ dimensions for the sample $\chi^{(k)}$ leads to a maximum number $N_{ph} = n_{ph}^M$ *phantom samples* in the augmented input space. The entire experimental design has then a size of $N \times n_{ph}^M$ samples.

The key feature of the phantom points is that they all correspond to the same $\chi^{(k)}$ in the original space, with associated model response $\mathcal{Y}^{(k)} = \mathcal{M}(\chi^{(k)})$. In other words, a *single run* of the model \mathcal{M} yields up to n_{ph}^M points in the augmented space.

An infinite number of phantom samples could be

generated in principle. In practice however, only a limited number is beneficial (see Section 5 and Figure 6).

5. APPLICATION

5.1. Rosenbrock function

The Rosenbrock function is a two-dimensional, smooth, polynomial function defined as (Rosenbrock, 1960):

$$\mathcal{M}(x_1, x_2) = 100(x_2 - x_1^2)^2 + (1 - x_1)^2. \quad (12)$$

The uncertainty associated with the two input variables $\{x_1, x_2\}$ is modelled by Gaussian random variables with interval-valued mean and standard deviation. For both variables, $\mu_{X_i} = [-0.5, 0.5]$ and $\sigma_{X_i} = [0.7, 1.0]$. Figure 2 shows the p-box of the input random variables as the region enclosed between solid lines.

The p-box of the response Y is obtained by applying the algorithm in Section 4. The p-box is interpreted as a parametric p-box for the nested Monte Carlo algorithm with and without meta-modelling (Section 4.2 and Section 4.1 respectively).

The experimental design consists of $N = 30$ Latin-hypercube samples generated from the parametric p-box described in Section 2.3. The imprecise parameters $\Theta_{\mathbf{X}}$ are interpreted as uniform random variables in order to cover the interval-valued $\theta \in \Theta_{\mathbf{X}}$ evenly. In the augmented space, $N_{ph} = 30$ phantom samples are used for each vector of the experimental design $\chi^{(k)} \in \mathcal{X}$, leading to a total number of samples in the experimental design of $N_{tot} = N \cdot N_{ph} = 900$ to build up the surrogate model in the augmented space of dimension $M_Z = 6$.

The N_{ph} phantom points for $\chi^{(k)}$ are obtained as follows: Assuming that $\mathbf{z}^{(k)} = [u_{1,1}^{(k)}, u_{2,1}^{(k)}, u_{3,1}^{(k)}, u_{1,2}^{(k)}, u_{2,2}^{(k)}, u_{3,2}^{(k)}]^T$. Through Latin-hypercube sampling N_{ph} samples are generated in the m -dimensional $\Theta_{\mathbf{X}}$ space, which defines the components $\{[u_{1,i}^{(k)}, u_{2,i}^{(k)}], i = 1, 2\}$. Then components $[u_{3,1}^{(k)}, u_{3,2}^{(k)}]$ are computed from Eq. (11).

The resulting p-boxes are shown in Figure 4 for both algorithms. Solid lines and the grey area represent the exact p-box of the output variable Y (double loop Monte Carlo simulation) whereas

diamonds represent the p-box from the surrogate model. Note that despite the small experimental design the exact response p-box and the meta-model based p-box match perfectly. This behaviour was expected since the computational model \mathcal{M} and the isoprobabilistic transform T are polynomial functions.

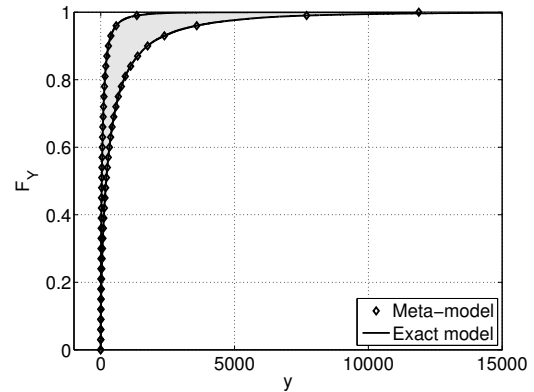


Figure 4: Rosenbrock function – comparing the resulting p-boxes for the exact model and the meta-model

5.2. Linear elastic truss

Consider the simply supported, linear-elastic truss presented in Hurtado (2013) and sketched in Figure 5. The computational model is a finite element model of a this truss structure. The Young's modulus of all bars is $E = 200 \cdot 10^9$ Pa whereas the cross section of the bars varies: 0.00535 m^2 for the bars marked by \bullet , 0.0068 m^2 for the bars marked by \circ and 0.004 m^2 for the remaining bars. The uncertainty in the input originates in the seven loads $\{P_i, i = 1, \dots, 7\}$ which are modelled as independent lognormal variables with mean value $\mu_{P_i} = [95, 105]$ kN and standard deviation $\sigma_{P_i} = [13, 17]$ kN (Hurtado, 2013). The quantity of interest is the deflection at midspan denoted by u_4 in Figure 5 as a function of the seven loads P_i .

An experimental design of $N = 100$ Latin-hypercube samples following a parametric p-box and varying number of phantom points N_{ph} is generated in a similar fashion as in Section 5.1. The total number of samples in the experimental design in the augmented input space is then $N_{tot} = N \cdot N_{ph} = 100 \cdot N_{ph}$.

Note that due to the lognormal distributions, Eq. (9) transforms into a function of the log-mean

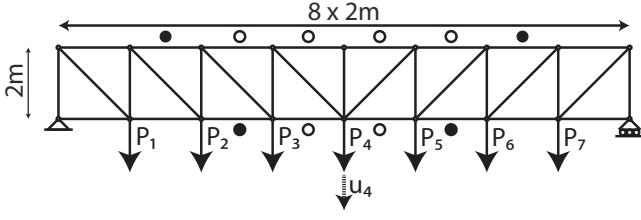


Figure 5: Truss structure – sketch of the geometry including the seven imprecise loads P_i and the target deflection u_4

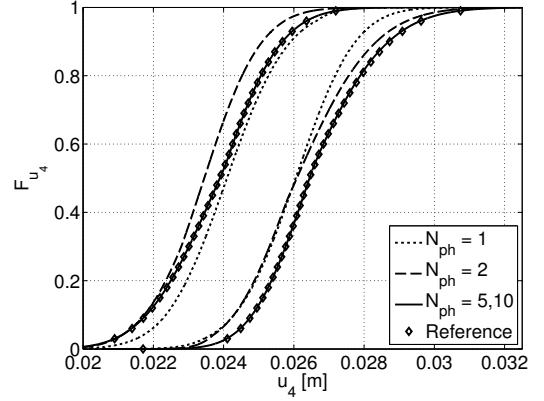


Figure 6: Truss structure – resulting p-boxes

λ and the log-standard deviation ζ for each load P (index $i = 1, \dots, 7$ has been omitted for clarity):

$$P = \exp[\lambda(U_1, U_2) + \zeta(U_1, U_2) \cdot U_3], \quad (13)$$

where $\zeta(U_1, U_2) = \sqrt{\ln(1 + (U_2/U_1)^2)}$, $\lambda(U_1, U_2) = \ln(U_1) - \zeta^2/2$, $U_1 = \mathcal{U}(95, 105)$ kN, $U_2 = \mathcal{U}(13, 17)$ kN and $U_3 = \mathcal{N}(0, 1)$. Hence, Eq. (11) transforms into:

$$u_{3,j}^{(k)} = \frac{\ln(p_j^{(k)}) - \lambda(u_{1,j}^{(k)}, u_{2,j}^{(k)})}{\zeta(u_{1,j}^{(k)}, u_{2,j}^{(k)})}. \quad (14)$$

Respecting the fact that the computational model for the beam deflection is a monotone function of the loads P_i , sampling the boundaries of the rectangular area defined by the ranges in $\{\mu_{P_i}, \sigma_{P_i}\}$ leads to the boundaries of the p-box of the output variable u_4 .

Figure 6 shows the boundaries of the p-box of the deflection variable u_4 for $n_{MC,1} = 10^3$ samples in the outer loop and $n_{MC,2} = 10^5$ samples in the inner loop of the nested Monte Carlo algorithm using the PC expansion in the augmented space. Positive values of u_4 correspond to a deflection direction indicated in Figure 5. The different line styles represent the number of phantom points ($N_{ph} = \{1, 2, 5, 10\}$). The reference p-box of the response u_4 is marked by diamonds which display a nested MC algorithm using the original finite element model with $10^3 \times 10^5$ runs.

The influence of the phantom points is clearly visible, since the p-boxes converge to a stable solution for an increasing number of phantom points. In this case stable solutions are obtained with $N_{ph} > 4$.

Note that when conducting a reliability analysis, the failure probability is given within the range provided by lower For instance $u_{4,adm} = 0.028$ m leads to a failure probability range of $P_f = \mathbb{P}(u_4 \geq u_{4,adm}) = [2.3 \cdot 10^{-3}, 1.8 \cdot 10^{-1}]$. Note that these results are obtained using only 100 finite element runs.

6. CONCLUSIONS

This paper deals with the propagation of uncertainty in the input of a computational model simulating a physical process. Due to sparsity of proper calibration data, the input parameters are modelled as imprecise probabilities, *i.e.* a combination of aleatory and epistemic uncertainties. This is a typical case in practice, where resources for generating data (*i.e.* measurements) are limited.

One way to capture this lack of knowledge are probability-boxes. Given parametric probability-boxes in the input variables, we propose an algorithm to propagate input uncertainty with the help of Polynomial Chaos Expansions. The use of parametric p-boxes allows for the separation of aleatory and epistemic uncertainty in the meta-model by introducing an augmented input space. Such separation is preserved in the p-box of the output variable of the system.

An essential part of the algorithm are phantom points which are artificial experimental design points generated in the augmented input space without the need of additional expensive exact model evaluations. They improve the accuracy of the meta-model without affecting computational re-

sources. This behaviour is due to the high redundancy of the augmented space formulation introduced to connect the p-boxes with PCE.

The capabilities of the proposed algorithm are shown on two examples: a benchmark analytical function and a more realistic engineering problem. In both cases the proposed algorithm is capable of predicting the response variable accurately with only a small number of exact computational model runs. This is of significance in practice where time, financial and computational resources are typically limited.

Further studies will include modifications of the proposed algorithm to accurately estimate small failure probabilities for which Monte Carlo simulation is not efficient. This will include the use of adaptive sampling algorithms for enriching experimental design continuously.

7. REFERENCES

- Berveiller, M., Sudret, B., and Lemaire, M. (2006). “Stochastic finite elements: a non intrusive approach by regression.” *Eur. J. Comput. Mech.*, 15(1-3), 81–92.
- Blatman, G. and Sudret, B. (2010). “An adaptive algorithm to build up sparse polynomial chaos expansions for stochastic finite element analysis.” *Prob. Eng. Mech.*, 25(2), 183–197.
- Blatman, G. and Sudret, B. (2011). “Adaptive sparse polynomial chaos expansion based on Least Angle Regression.” *J. Comput. Phys.*, 230, 2345–2367.
- Chowdhary, K. and Dupuis, P. (2013). “Distinguishing and integrating aleatoric and epistemic variation in uncertainty quantification.” *ESAIM Math. Model. Numer. Anal.*, 47(3), 635–662.
- Dempster, A. P. (1967). “Upper and lower probabilities induced by multivalued mapping.” *Ann. Math. Stat.*, 38(2), 325–339.
- Efron, B., Hastie, T., Johnstone, I., and Tibshirani, R. (2004). “Least angle regression.” *Ann. Stat.*, 32, 407–499.
- Eldred, M. S. and Swiler, L. P. (2009). “Efficient algorithms for mixed aleatory-epistemic uncertainty quantification with application to radiation-hardened electronics part I : algorithms and benchmark results.” *Report No. SAND2009-5805*, Sandia National Laboratories.
- Ferson, S. and Ginzburg, L. R. (1996). “Different methods are needed to propagate ignorance and variability.” *Reliab. Eng. Sys. Safety*, 54(2-3), 133–144.
- Ferson, S. and Hajagos, J. G. (2004). “Arithmetic with uncertain numbers: rigorous and (often) best possible answers.” *Reliab. Eng. Sys. Safety*, 85(1-3), 135–152.
- Gelman, A. (2006). “Prior distributions for variance parameters in hierarchical models (comment on article by Browne and Draper).” *Bayesian Anal.*, 1(3), 515–534.
- Ghanem, R. and Spanos, P. (2003). *Stochastic Finite Elements : A Spectral Approach*. Courier Dover Publications.
- Gunn, S. (1998). “Support vector machines for classification and regression.” *Report No. ISIS-1-98*, Dpt. of Electronics and Computer Science, University of Southampton.
- Hurtado, J. E. (2013). “Assessment of reliability intervals under input distributions with uncertain parameters.” *Prob. Eng. Mech.*, 32, 80–92.
- Rosenbrock, H. (1960). “An automatic method for finding the greatest or least value of a function.” *Comput. J.*, 3, 175–184.
- Santner, T. J., Williams, B. J., and Notz, W. I. (2003). *The Design and Analysis of Computer Experiments*. Springer, New York.
- Shafer, G. (1976). *A mathematical theory of evidence*. Princeton University Press, Princeton, NJ.
- Sudret, B. (2007). *Uncertainty propagation and sensitivity analysis in mechanical models – Contributions to structural reliability and stochastic spectral methods*. Université Blaise Pascal, Clermont-Ferrand, France. Habilitation à diriger des recherches, 173 pages.
- Sudret, B. (2014). “Polynomial chaos expansions and stochastic finite element methods.” *Risk Reliab. Geotech. Eng.*, K. K. Phoon and J. Ching, eds., Taylor and Francis, Chapter 6.